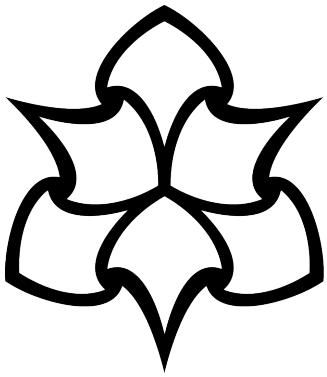

A simple model predicts energetically optimised jumping in dogs

Katherine A J Daniels and J F Burn

Queen's School of Engineering, University of Bristol

Corresponding author's email address: k.daniels@bristol.ac.uk (K.A.J. Daniels)

Key words: locomotion, jumping, energetics, optimisation, biomechanics

SUMMARY STATEMENT

A simple model of jumping mechanics is used to show that domestic dogs use complex anticipatory control to systematically choose jump trajectories close to those that minimise mechanical energy.

ABSTRACT

It is generally accepted that animals move in a way that minimises energy use during regular gait and there is evidence that the principle might extend more generally to locomotor behaviour and manoeuvres. Jumping during locomotion is a useful manoeuvre that contributes to the versatility of legged locomotion and is within the repertoire of many terrestrial animals. We describe a simple ballistic model that can be used to identify a single unique trajectory of the body's centre of mass that minimises the mechanical work to initiate a jump, regardless of the approach velocity or take-off position. The model was used to show that domestic dogs (*Canis lupus familiaris*) demonstrate complex anticipatory control of locomotor behaviour by systematically using jump trajectories close to those that minimised the mechanical energy of jumps over raised obstacles. It is unclear how the dogs acquired the complex perception and control necessary to exhibit the observed behaviour. The model may be used to investigate whether animals adopt energetically optimised behaviour in any similarly-constrained ballistic task.

INTRODUCTION

It is generally accepted that, in the absence of other imperatives, animals minimise the energy used for locomotion. Evidence from a range of investigations indicates that animals adopt speeds (Ralston, 1958; Hoyt and Taylor, 1981), step length-frequency combinations (Zarrugh et al., 1974; Zarrugh and Radcliffe, 1978; Cavagna and Franzetti, 1986; Minetti and Saibene, 1992; Minetti et al., 1995), step widths (Donelan et al., 2001), and gaits (Hoyt and Taylor, 1981; Alexander, 1984; Griffin et al., 2004) similar to those that minimise the net cost of transport when travelling over flat, level ground. The natural environment of terrestrial animals, however, is typically not uniformly flat but contains obstacles, for example holes, steps, rocks and vegetation. Animals that encounter obstacles in the path of travel must either re-route to avoid them or execute a manoeuvre such as jumping to traverse the obstacle. There is evidence that the principle of minimising energy use might extend beyond the physiology of locomotion to locomotor behaviours (Minetti, 1995) and beyond regular gait to manoeuvres (Moraes and Patla, 2006).

Jumping over an obstacle in the path of travel during locomotion is a manoeuvre in the locomotor repertoire of many species of terrestrial animal. It allows traversal of a raised obstacle or a length of ground without physical contact, change of direction or significant reduction in forward velocity but at the cost of raising the body centre of mass (CoM). The manoeuvre has been studied extensively in species that use jumping as a mode of progression (e.g. Marsh and John-Alder 1994; Peplowski and Marsh 1997; Aerts 1998; Azizi and Roberts 2010) and there is a sizable literature relating to its use in the athletic pursuits of humans and horses (e.g. Alexander 1990; Hay 1993; Seyfarth et al. 2000; Dutto et al. 2004; Bobbert and Santamaría 2005). The focus for much of this work has been on the anatomical mechanisms and physiological processes that allow animals to produce the high power required for the exceptional performance observed in some species. Whether animals control the manoeuvre to minimise energy use is not known.

Although jumping is an inherently costly manoeuvre, the mechanical work required to jump over an obstacle depends on the trajectory followed. Consider a simple obstacle formed from a raised horizontal bar at a fixed distance from a defined take-off position. Any one of a theoretically-infinite number of trajectories could be used to pass over the obstacle with minimum adequate clearance; only a single unique trajectory, however, would minimise overall mechanical energy. Both horses and dogs use jump trajectories that differ depending on the size and shape of the obstacle being traversed (Pfau et al., 2011; Birch et al., 2016; Lewczuk et al., 2007), suggesting that they might have the capacity to control take-off to follow an energetically optimum trajectory.

We hypothesised that domestic dogs (*Canis lupus familiaris*) would utilise trajectories that minimised the mechanical work done during the take-off stride when jumping over a raised obstacle from a constrained take-off position. The optimum jump trajectory was predicted based on the height of the obstacle and the horizontal distance from the obstacle at take-off. The predicted trajectories were then compared with the trajectories recorded for dogs when jumping, over a large range of constrained take-off distances.

MATERIALS AND METHOD

MODEL DESCRIPTION

A simple planar model was developed to calculate the mechanical energy required at the instant of take-off for the traversal of a raised obstacle.

Consider a point mass launched from the origin in an upwards and forwards direction such that its ballistic trajectory passes over a height constraint located at distance d and height h from the origin (Figure 1). Assuming energy loss due to aerodynamic drag is negligible, the mechanical energy of the mass E_{mech} is constant throughout flight and can be defined in terms of the location of the apex (x, y) of the trajectory thus,

$$E_{mech} = GPE + KE = mgy + \frac{mx^2 g}{4y} \quad (1)$$

where GPE and KE refer to gravitational potential and kinetic energy respectively and g is gravitational acceleration.

In Figure 2 the energy associated with ballistic trajectories that pass over the height constraint are plotted as a function of apex position at a spatial resolution of 10 mm. Although there are an infinite number of trajectories that would pass over the height constraint, their apices within the space defined by the axes of Figure 2 are constrained to the region shown. Due to symmetry, the x coordinate of the apex must be $> d/2$. It can be observed that there exists a single, unique trajectory that minimises the energy required to pass over the height constraint. The optimisation arises due to the trade-off between maximum GPE gained and KE due to velocity in the direction of travel. The trade-off is apparent from Equation 1 in which the GPE increases and KE decreases with increasing y. It can be shown analytically that a single minimum exists for any combination of h and d, $(h, d > 0)$.

We applied this simple model to the energetics of jumping manoeuvres used by dogs during locomotion as follows:

1. The trajectories of jumps made by dogs were represented using a Cartesian reference frame in which horizontal distance in the direction of travel was represented on the x axis and vertical distance or height was represented on the y axis. We assumed that motion outside this x-y plane was negligible. Ground level was defined as y = 0.
2. An obstacle in the form of a horizontal raised bar over which dogs jumped was modelled as a height constraint as described above. The location of the obstacle was used to define x = 0 with x increasing in the direction of travel (Figure 3). Hence the intersection with ground-level of a line projected vertically downwards from the obstacle defined the origin of the reference frame.
3. The location and mass of the dog were represented by a single point mass equal to body mass and coincident with the location of the body CoM.
4. Take-off was defined as the instant at which the animal lost contact with the ground at the onset of jump aerial phase.
5. The effect of aerodynamic drag was assumed to be negligible and so the horizontal component of velocity (v_x) was assumed constant throughout ballistic flight.
6. The contribution of angular kinetic energy of the body to the total mechanical energy was relatively insignificant and not incorporated into the model. Estimation of angular kinetic energy based on the morphometric data of Fedak et al. (1982) suggested that this component comprised <7 % of the energy cost of a jump.
7. Approach velocity $v0_x$ was defined as the mean horizontal velocity of the ultimate stride before take-off.
8. Jump length was approximated as twice the horizontal distance travelled by the CoM between take-off and apex location.

In the context of jumping during locomotion, kinetic energy associated with approach velocity (see 7 above) contributes to the kinetic energy at the point of take-off. We hypothesised that animals would choose a trajectory that minimised the energy *added* during the take-off stride regardless of approach velocity. Thus the cost function E_{mech+} used to find the minimum energy trajectory was evaluated as the energy of the jump trajectory (E_{mech} , Equation 1) minus the kinetic energy due to approach velocity. It was observed in the experimental data that the horizontal velocity during the jump was always greater than approach velocity. The mechanical cost of transport based on energy added at take-off C_{mech+} was defined as the mechanical energy added at take-off E_{mech+} divided by jump length. Mass-specific values of these parameters were obtained by dividing by body mass.

The parameters defined in Figure 3 were obtained using motion capture for each jump performed by a group of dogs over a set of obstacle positions. Our approach was to compare the measured trajectory defined in terms of apex position with the optimum trajectory modelled as the apex position that minimised E_{mech+}. The optimum trajectory was obtained numerically by evaluating the energy required for potential apex positions at a spatial resolution of 10 mm. Calculations were performed in MATLAB (R2009a, MathWorks, MA, USA) using the following formulae:

Assume we wish to model the energetics of an apex position of (a_x, a_y) given a take-off position of (d_x, d_y) and an obstacle height b_y. The fundamental constraint on the dynamics of the jump is the time t taken to reach the apex location from take-off, which is determined by the acceleration due to gravity g.

$$t = \sqrt{\frac{2(a_y - d_y)}{g}} \tag{2}$$

The horizontal component of velocity during the jump is thus constrained to be that required to reach the horizontal location of the apex in time t.

$$v_x = \frac{(a_x - d_x)}{t} \tag{3}$$

The energy added at take-off E_{mech+} can be calculated either as the difference between the KE of CoM at take-off and the KE due to approach velocity or, equivalently, the GPE gained in raising the CoM to the apex height plus the difference between the KE due to forward movement during the jump and the KE due to forward movement during the approach. The mechanical cost of transport C_{mech+} was calculated as E_{mech+} divided by jump length. Mass-specific values of energy and cost were also calculated,

$$\frac{E_{mech+}}{m} = g(a_y - d_y) + \frac{1}{2}(v_x^2 - v0_x^2) \tag{4}$$

$$\frac{C_{mech+}}{m} = \frac{E_{mech+}}{2mv_x t} \tag{5}$$

where $v0_x$ is approach velocity, v_x is the horizontal component of velocity during the jump and m is body mass. The condition for the trajectory to pass over the obstacle depends on the horizontal position of the apex relative to the obstacle. Three possibilities exist:

1. If the horizontal positions of the apex and obstacle are coincident ($a_x = 0$) then the condition for success is that apex height is greater than obstacle height ($a_y > b_y$).

2. If the horizontal position of the apex is before the obstacle ($a_x < 0$) then the condition for success is that the time for the CoM to fall to obstacle height must be greater than the time to reach the obstacle from the apex position

$$\frac{0 - a_x}{v_x} < \sqrt{\frac{2(a_y - b_y)}{g}}$$

3. If the horizontal position of the apex is after the obstacle ($a_x > 0$) then the condition for success is that the time for the CoM to increase height from take-off height to obstacle height must be less than time to reach the obstacle.

$$\frac{a_x - d_x}{v_x} < \sqrt{\frac{2(a_y - d_y)}{g}} - \sqrt{\frac{2(a_y - b_y)}{g}}$$

Examples of trajectories that minimise E_{mech+}/m and C_{mech+}/m for the take-off position and height constraint used for Figures 1 and 2 are shown in Figure 4.

The model so far described has considered the CoM passing over the obstacle as the condition for successful traversal. In reality the entirety of the body, within which a jumping dog's CoM is located, must pass over the obstacle without making contact. The minimum possible height of the CoM at the instant when it is vertically above the obstacle (x=0; indicated as point c in Figure 5A) must thus be the sum of obstacle height and vertical distance from the CoM to the ventral surface of the animal's thorax. This parameter, the minimum height that must be reached by the CoM for a successful traversal, is termed *effective obstacle height* (*EOH*; Figure 5B). An example E_{mech+}/m optimisation showing the additional constraint imposed by the body is shown in Figure 5A. Increasing the height by which the CoM must be raised between take-off and crossing the obstacle (EOH - d_y) shifted the optimum apex position in the direction of travel (positive x) and in the upwards (positive y) direction, whilst increasing $v0_x$ or d_x shifted the optimum apex position in the direction of travel and in the downwards (negative y) direction. For initial conditions within the experimentally-observed range, a different but similar trajectory minimised C_{mech+}/m.

EXPERIMENTAL DATA COLLECTION

Data were collected from five dogs (Table 1). Ethical approval for the study protocol was provided by the University of Bristol Animal Services Unit. The cranio-caudal position of the CoM during standing was measured directly in dogs P1, P2 and P3 using a balance board. The identified CoM location relative to anatomical landmarks in these dogs was used to estimate cranio-caudal CoM position in P4 and P5, neither of whom would stand still enough for a reliable measurement to be made. The dorso-ventral position of the CoM was estimated in all dogs as the midpoint of a vertical line drawn on the surface of the trunk between the dorsal and ventral midlines at the cranio-caudal position of the CoM while the dog was standing. A retro-reflective marker was placed on the lateral trunk at the position of the CoM. Markers were also placed on the feet to allow the instant of take-off to be identified.

An *obstacle* was constructed on a 12 m long track in a gait laboratory. The obstacle comprised a single raised bar (the *obstacle bar*) and a variable number of *base bars* which were laid on the track surface on the approach side of and parallel to the obstacle bar. The base bars were used to constrain the minimum distance in front of the obstacle bar (*obstacle length*) from which the dogs could take off when jumping over the obstacle (Figure 5B). The height of the obstacle was set for each dog to be comfortably traversable from a range of take-off positions. Each dog jumped obstacles of a range of lengths presented in ascending order (Table 2) whilst kinematic data were recorded at 200 fps using an optical motion capture system (Oqus, Qualisys AB, Gothenburg, Sweden).

CoM position at take-off (d_x, d_y), CoM apex position (a_x, a_y) and approach velocity ($v0_x$) were recorded for each trial, where $v0_x$ was defined as the mean horizontal velocity of the CoM in the ultimate stride before take-off. Take-off was identified as the first frame of the obstacle traversal stride in which no part of the animal was in contact with the ground. *EOH* was calculated for each dog by summing of the height of the obstacle bar and the vertical distance from the ventral surface of the dog's trunk to the CoM marker during standing (Figure 1A). *EOH* was used as the obstacle height (b_y) input to the model.

ANALYSIS

For each trial, the CoM position at take-off (d_x, d_y), and the *EOH* (0, b_y) were used to predict the apex position (a_x, a_y) of the unique trajectories that would minimise E_{mech+}/m and C_{mech+}/m for the jump. The corresponding apex position in the experimental data was identified as the position at which the CoM marker attained maximum height. The E_{mech+}/m associated with the measured trajectory was calculated from take-off velocity, and C_{mech+}/m was obtained by dividing E_{mech+}/m by twice the

horizontal distance travelled by the CoM between take-off and apex location. Measured and predicted values of a_x and a_y were divided by *EOH* to calculate dimensionless parameters (*relative apex position)* $\hat{a}_x$ and $\hat{a}_y$ for comparison across dogs. The model was evaluated by plotting measured values of $\hat{a}_x$, $\hat{a}_y$ against predicted values that optimised E_{mech+}/m and C_{mech+}/m respectively. Measured values of the two energetic parameters were also plotted against their predicted optimum values. Linear regression models were fitted to the data in each plot and the residuals examined to evaluate appropriateness of the fitted model. Hypothesis tests of the regression models against the line $y=x$ were used to evaluate statistically the deviation from the predicted values. Values of r^2 were used to indicate the proportion of linear variation in measured parameters that may be attributed to variation in their predicted value.

RESULTS

A total of 62 trials were collected from 5 dogs. All dogs performed 12 trials each except for subject P2 who performed 14 trials.

Experimentally modifying the obstacle length caused changes in d_x and hence in the predicted optimum trajectories. For all trials the measured positions of the trajectory apices were close to those predicted for least mechanical energy and least mechanical cost of transport (Figure 6A, B, D, E). Dogs systematically changed their apex position as predicted by the model in response to changes in obstacle length: as obstacle length increased jump CoM apices became higher and horizontally more distant from the obstacle bar (see Figures S1 and S2 in Electronic Supplementary Material for all individual results). In all cases linear models were appropriate for the data. Changes in predicted values if minimising E_{mech+}/m accounted for 72% of the measured variation in $\hat{a}_x$,39% of the measured variation in relative $\hat{a}_y$ and 71% of the measured variation in E_{mech+}/m (Figure 6A-C). The empirical models for $\hat{a}_x$ and $\hat{a}_y$ data did not deviate significantly from the theoretical model ($\hat{a}_x$, $p = 0.91$; $\hat{a}_y$, $p = 0.06$ (intercept) and $\hat{a}_x$, $p = 0.25$; $\hat{a}_y$, $p = 0.17$, (slope)). Changes in predicted values if minimising C_{mech+}/m accounted for 72% of the measured variation in $\hat{a}_x$,41% of the measured variation in relative $\hat{a}_y$ and 66% of the measured variation in C_{mech+}/m (Figure 6D-F). The empirical models for $\hat{a}_x$ and $\hat{a}_y$ data did not deviate significantly from the theoretical model ($\hat{a}_x$, $p = 0.52$, $\hat{a}_y$, $p = 0.06$ (intercept) and $\hat{a}_x$, $p= 0.14$, $\hat{a}_y$, $p = 0.18$, (slope)). The empirical models for E_{mech+}/m *and* C_{mech+}/m differed significantly in intercept, ($p < 0.01$ and $p < 0.01$ respectively) and slope ($p < 0.01$ and $p < 0.03$) from the theoretical model predictions.

There was no significant relationship between $v0_x$ and obstacle length. A trend towards a small positive relationship was observed although not significant at $\alpha = 0.05$ ($p = 0.06$). Dogs did not thus appear to be strongly regulating approach speed for the jump and the systematic change in the horizontal component of jump velocity with obstacle length may be assumed to originate largely from the take-off rather than from the approach.

DISCUSSION

The aim of the experiment was to provide evidence that the dogs used a control law for jumping that minimised external work. In controlling take-off position the experimental design equated the minimisation of work to the selection of a unique ballistic trajectory which could easily be measured from the kinematics of the body CoM. Estimation of CoM position was inevitably the largest potential source of error in the collection of experimental data. Given the inter-breed variability in dog morphology and the lack of appropriate morphometric data it is unlikely that using a dynamic estimate based on a multi-segment model (Amit et al., 2009; Nielsen et al., 2003; Colborne et al., 2005) would have improved the accuracy. Using the method for estimating CoM position described in Channon et al. (2012) excluding the distal limbs, for comparison, we found negligible non-systematic differences in measured/optimal $\hat{a}_x$ and $\hat{a}_y$ of <0.1 and <0.04 respectively with an effect on E_{mech+}/m of <0.15 Jkg^{-1}. By changing the take-off position over a relatively large range the expected systematic change in the position of the CoM at the apex of the ballistic trajectory was much greater than the uncertainty in the measurement of CoM position and the effect was clearly apparent in the data.

The empirical models for $\hat{a}_x$ and $\hat{a}_y$ were not significantly different from the theoretical predictions for minimum energy and for minimum cost. There was evidence of a small bias towards greater measured than predicted values, especially for $\hat{a}_y$, and a trend towards a smaller slope (Figures 6A, B, D, E), but these may be attributed at least in part to the dogs including a safety margin in their clearance of the obstacle. Our theoretical prediction was based on the absolute minimum height to pass above the obstacle not including any additional clearance. The relative size of the bias on $\hat{a}_x$ and $\hat{a}_y$ suggests that clearance was achieved mostly by an increase in apex height.

The empirical models for E_{mech+}/m and C_{mech+}/m differed significantly from the theoretical predictions, but as these parameters were constructed from the data for $\hat{a}_y$ and the square of the data for $\hat{a}_x$ the statistical difference is perhaps unsurprising. In absolute terms the difference between the theoretical and empirical models resulted from differences in apex position of the order of a few centimetres and comparable to the magnitude of uncertainty of CoM position. The clustering of C_{mech+}/m data (Figure 6F) data for some individual dogs may be explained by the correlation between potential energy gain and jump distance for those dogs. We note, however, that the slope of the regression model for C_{mech+}/m was dominated by data from a single dog and there was a relatively large amount of random variation on the data for another. We conclude that the data do not show that the dogs behaved consistently to minimise C_{mech+}/m. In contrast, the data for E_{mech+}/m (Figure 6C) indicate consistent behaviour of all dogs with the variation in theoretical predictions explaining 71% of the variation in the measured values. We propose that it is unlikely that dogs would have exhibited this behaviour of anything close to it were it not to minimise the work of jumping or some closely related energetic parameter: it differed considerably from the behaviour required to minimise the height gained by the CoM during the jump, which would have also minimised added GPE and required that the apex position was invariant above the obstacle (i.e. at x = 0 in Figure 2, and in middle row panels of Figures S1 and S2). We conclude that dogs closely followed trajectories that minimised E_{mech+}/m.

One might reasonably assume that a selection pressure to minimise energy use would act to reduce metabolised energy and not mechanical work (Alexander, 1989). Both would be strongly correlated if muscle efficiency and the elastic strain energy exchanges remained fairly constant across the range of jumps performed but that cannot be assumed. Neither can we exclude the possibility that the observed optimisation is a secondary correlate to a closely-related target parameter such as power.

We propose that a notable feature of our model is that it allows an absolute prediction of a unique expected behaviour based on very few assumptions, which minimises an energetic parameter.

Most of the evidence for energetic optimisation of locomotion is based on either the free selection of a behaviour shown empirically to minimise metabolic cost, or the observation that experimentally imposed changes to preferred locomotor behaviour result in increased cost. The theoretical basis for empirically determined cost minima is as yet incomplete.

Successful obstacle traversal requires anticipatory control based on remote sensing using vision (Mohagheghi et al., 2004). It is unclear how the dogs acquired the complex perception and control necessary to exhibit the behaviour observed in this study. It is unlikely that any of the dogs would have encountered obstacles of similar geometry during their everyday activity or with the frequency for skill acquisition through practice. In some measure the behaviour might be innate and part of an extended phenotype for the species. We note that it is a remarkable example of the effectiveness of vision-based anticipatory control and raises the possibility that other similar constrained ballistic tasks might be optimised in the same way.

COMPETING INTERESTS

No competing interests declared.

FUNDING

Financial support was provided by the Engineering and Physical Sciences Research Council (Doctoral Training Grant to K.A.J.D.) and the Wellcome Trust (equipment grant to Bristol Vision Institute).

DATA AVAILABILTY

Data are provided as electronic supplementary material.

REFERENCES

Aerts, P. (1998). Vertical jumping in Galago senegalensis: the quest for an obligate mechanical power amplifier. *Proc. Royal Soc. B.* **353**, pp. 1607–1620.

Alexander, R.M. (1989). Optimization and gaits in the locomotion of vertebrates. *Physiol. Rev.* **69**(4), pp. 1199–1227.

Alexander, R.M. (1990). Optimum take-off techniques for high and long jumps. *Proc. Royal Soc. B.* **329**, pp. 3–10.

Alexander, R.M. (1984). The gaits of bipedal and quadrupedal animals. *Int. J. Rob. Res.* **3**(2), pp. 49–59.

Amit, T., Gomberg, B.R., Milgram, J. and Shahar, R. (2009). Segmental inertial properties in dogs determined by magnetic resonance imaging. *Vet. J.* **182**(1), pp. 94–9.

Azizi, E. and Roberts, T.J. (2010). Muscle performance during frog jumping: influence of elasticity on muscle operating lengths. *Proc. Royal Soc. B.* **277**, pp. 1523–30.

Birch, E., Carter, A. and Boyd, J. (2016). An examination of jump kinematics in dogs over increasing hurdle heights. *Comp. Exerc. Physiol.* **12**(2), pp. 91–98.

Bobbert, M.F. and Santamaría, S. (2005). Contribution of the forelimbs and hindlimbs of the horse to mechanical energy changes in jumping. *J. Exp. Biol.* **208**, pp. 249–60.

Cavagna, G.A. and Franzetti, P. (1986). The determinants of the step frequency in walking in humans. *J. Physiol.* **373**, pp. 235–242.

Channon, A.J., Usherwood, J.R., Crompton, R.H., Günther, M.M. and Vereecke, E.E. (2012). The extraordinary athletic performance of leaping gibbons. *Biol. Lett.* **8**, pp. 46–49.

Colborne, G.R., Innes, J.F., Comerford, E.J., Owen, M.R. and Fuller, C.J. (2005). Distribution of power across the hind limb joints in Labrador Retrievers and Greyhounds. *Am. J. Vet. Res.* **66**(9), pp. 1563–71.

Donelan, J.M., Kram, R. and Kuo, A.D. (2001). Mechanical and metabolic determinants of the preferred step width in human walking. *Proc. Royal Soc. B.* **268**, pp. 1985–92.

Dutto, D.J., Hoyt, D.F., Clayton, H.M., Cogger, E.A. and Wickler, S.J. (2004). Moments and power generated by the horse (Equus caballus) hind limb during jumping. *J. Exp. Biol.* **207**(4), pp. 667–674.

Fedak, M.A., Heglund, N.C. and Taylor, C.R. (1982). Energetics and mechanics of terrestrial

locomotion. II. Kinetic energy changes of the limbs and body as a function of speed and body size in birds and mammals. *J. Exp. Biol.* **97**, pp. 23–40.

Griffin, T.M., Kram, R., Wickler, S.J. and Hoyt, D.F. (2004). Biomechanical and energetic determinants of the walk-trot transition in horses. *J. Exp. Biol.* **207**, pp. 4215–23.

Hay, J., (1993). Citius, altius, longius (faster, higher, longer): the biomechanics of jumping for distance. *J. Biomech.* **26**(S1), pp. 7–21.

Hoyt, D.F. and Taylor, C.R. (1981). Gait and the energetics of locomotion in horses. *Nature* **292**(16), pp. 239–40.

Lewczuk, D., Wejer, J. and Sobieraj, D. (2007). Analysis of angles of taking off, landing, and work of limbs in horses jumping above the spread obstacle of different structure. *Anim. Sci. Pap. Reports* **25**(4), pp. 297–304.

Marsh, R.L. and John-Alder, H.B. (1994). Jumping performance of hylid frogs measured with high-speed cine film. *J. Exp. Biol.* **188**, pp. 131–41.

Minetti, A.E. (1995). Optimum gradient of mountain paths. *J. Appl. Physiol.* **79**(5), pp. 1698–703.

Minetti, A.E., Capelli, C. and Zamparo, P. (1995). Effects of stride frequency on mechanical power and energy expenditure of walking. *Med. Sci. Sport Exerc.* **27**(8), pp. 1194–1202.

Minetti, A.E. and Saibene, F. (1992). Mechanical work rate minimization and freely chosen stride frequency of human walking: a mathematical model. *J. Exp. Biol.* **170**, pp. 19–34.

Mohagheghi, A.A., Moraes, R. and Patla, A.E. (2004). The effects of distant and on-line visual information on the control of approach phase and step over an obstacle during locomotion. *Exp. Brain Res.* **155**(4), pp. 459–68.

Moraes, R. and Patla, A.E. (2006). Determinants guiding alternate foot placement selection and the behavioral responses are similar when avoiding a real or a virtual obstacle. *Exp. Brain Res.* **171**(4), pp. 497–510.

Nielsen, C., Stover, S., Schultz, K.S., Hubbard, M. and Hawkins, D.A. (2003). Two-dimensional link-segment model of the forelimb of dogs at a walk. *Am. J. Vet. Res.* **64**(5), pp. 609–17.

Peplowski, M.M. and Marsh, R.L. (1997). Work and power output in the hindlimb muscles of Cuban tree frogs Osteopilus septentrionalis during jumping. *J. Exp. Biol.* **200**, pp. 2861–70.

Pfau, T., Garland de Rivaz, A., Brighton, S. and Weller, R. (2011). Kinetics of jump landing in agility dogs. *Vet. J.* **190**(2), pp. 278–83.

Ralston, H.J. (1958). Energy expenditure of normal human subjects during walking. *Fed. Proc.* **17**(1), p. 127.

Seyfarth, A., Blickhan, R. and Van Leeuwen, J.L. (2000). Optimum take-off techniques and muscle design for long jump. *J. Exp. Biol.* **203**, pp. 741–50.

Zarrugh, M.Y. and Radcliffe, C.W. (1978). Predicting metabolic cost of level walking. *Eur. J. Appl. Physiol. Occup. Physiol.* **38**(3), pp. 215–223.

Zarrugh, M.Y., Todd, F.N. and Ralston, H.J. (1974). Optimization of energy expenditure during level walking. *Eur. J. Appl. Physiol. Occup. Physiol.* **33**(4), pp. 293–306.

FIGURES

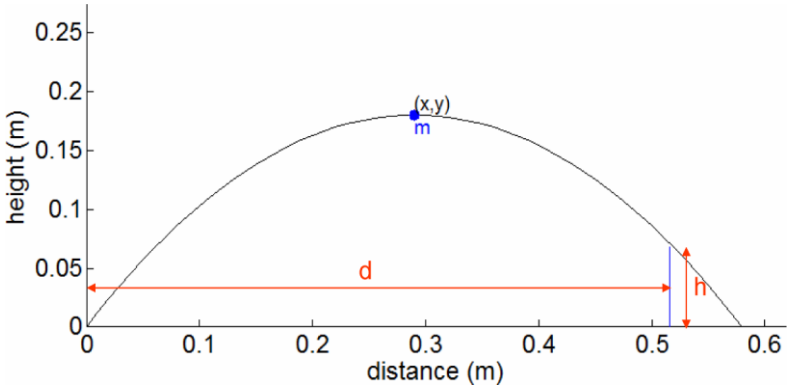

Figure 1: **A ballistic trajectory with apex at (*x*, *y*) passing over a height constraint at distance *d* and height *h* from the origin.**

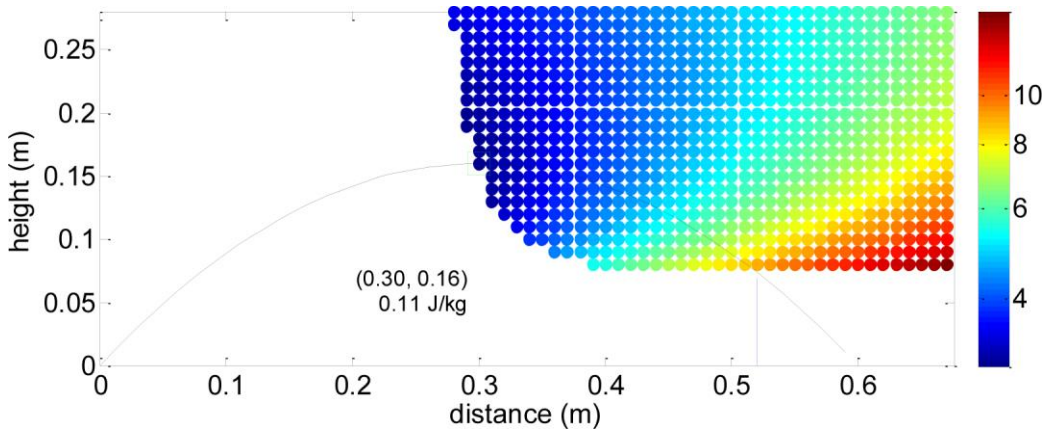

Figure 2: **Coloured dots at a spatial resolution of 10 mm represent the apex positions and associated energy of trajectories that pass over the height constraint.** The colour scale bar is marked in Jkg^{-1}. The minimum-energy trajectory is drawn in black with the apex position (0.30, 0.16) marked by a green square.

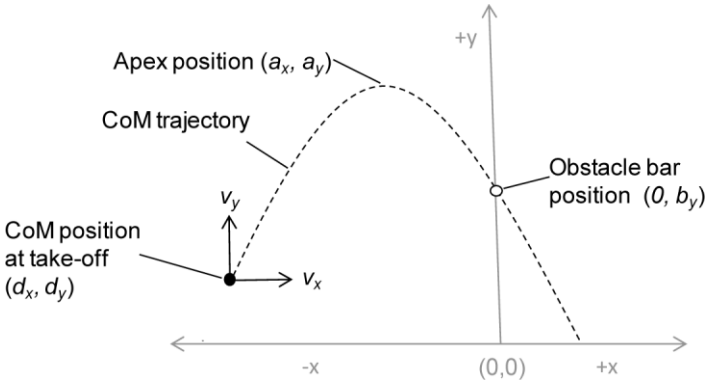

Figure 3: **The model applied to jumping.** Lateral view of CoM and obstacle at instant of take-off showing the trajectory of the CoM for a given take-off position (d_x, d_y) and apex position (a_x, a_y). Not to scale.

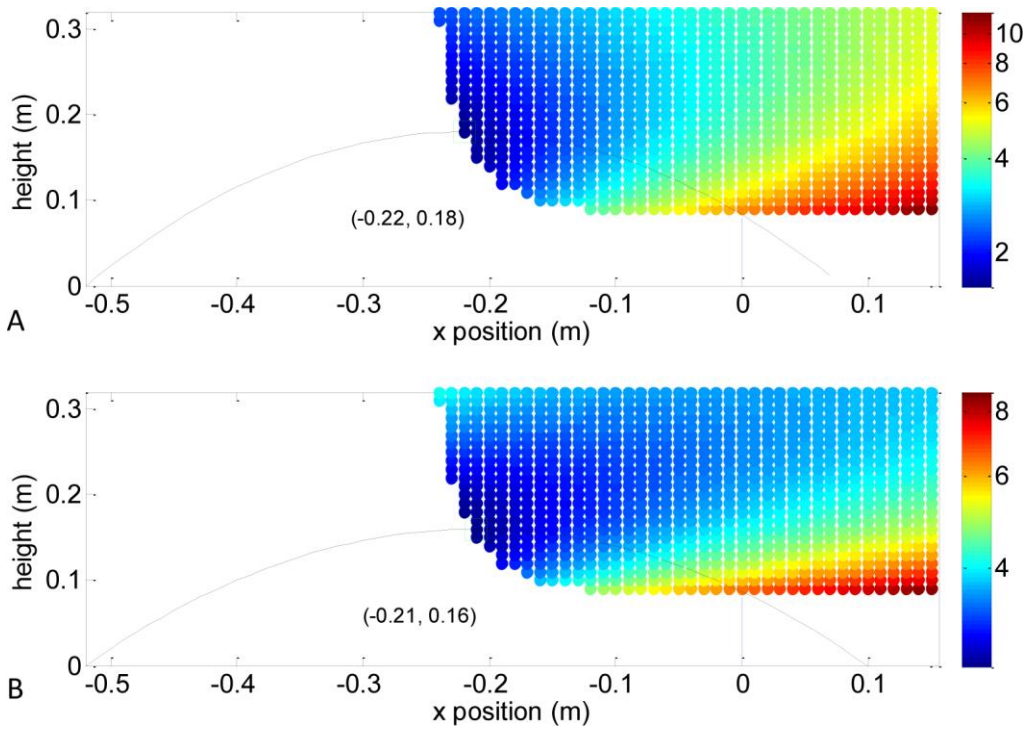

Figure 4: **Trajectories that minimise E_{mech+}/m (A) and C_{mech+}/m (A) with approach speed 1.7 ms^{-1}.** Height (y axis) is referenced to CoM height at the instant of take-off. The colour scale bar is marked in Jkg^{-1} (A); Jkg^{-1}m^{-1} (B). The trajectory that minimises each parameter is drawn in black with the apex position marked by a green square.

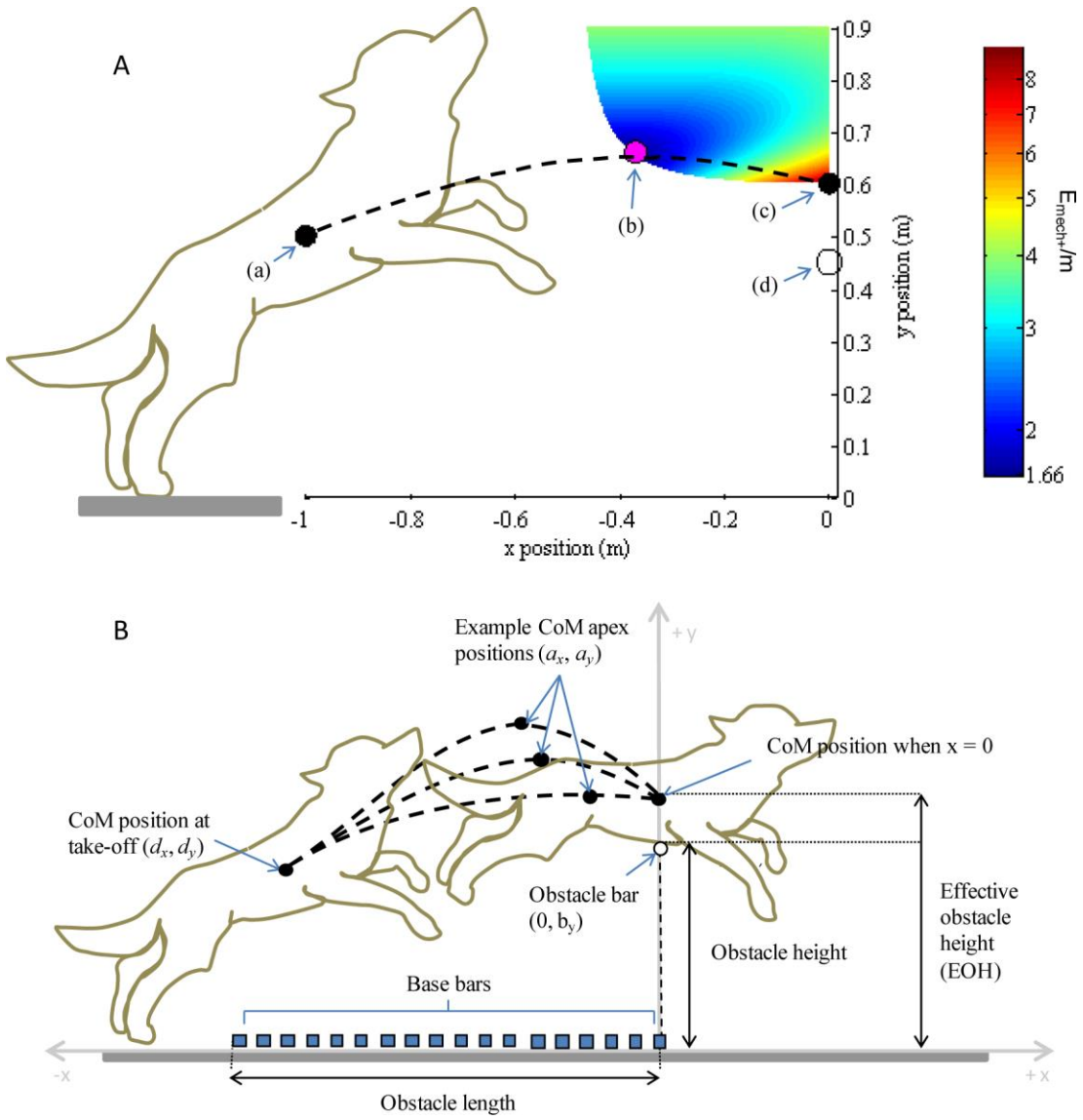

Figure 5: **Lateral view of an obstacle traversal.** A) Example optimisation for approximately mean take-off conditions across all dogs and trials (*EOH* = 0.6 m, d_x = -1 m, d_y = 0.5 m and $v0_x$ = 3 ms^{-1}). (a) indicates the position of the CoM of the dog at the instant of take-off and (c) indicates the position of the CoM as it passes over the obstacle bar (d) with clearance zero. The colour plot shows the distribution of E_{mech+}/m (Jkg^{-1}) for all successful trajectory apex positions within the graphed solution space (i.e. all trajectories in which the CoM would pass over (c)). A single energetically optimum CoM apex position exists and is indicated as a magenta circle (b). The associated CoM trajectory is shown as a broken line. B) Experimental set-up and measured parameters.

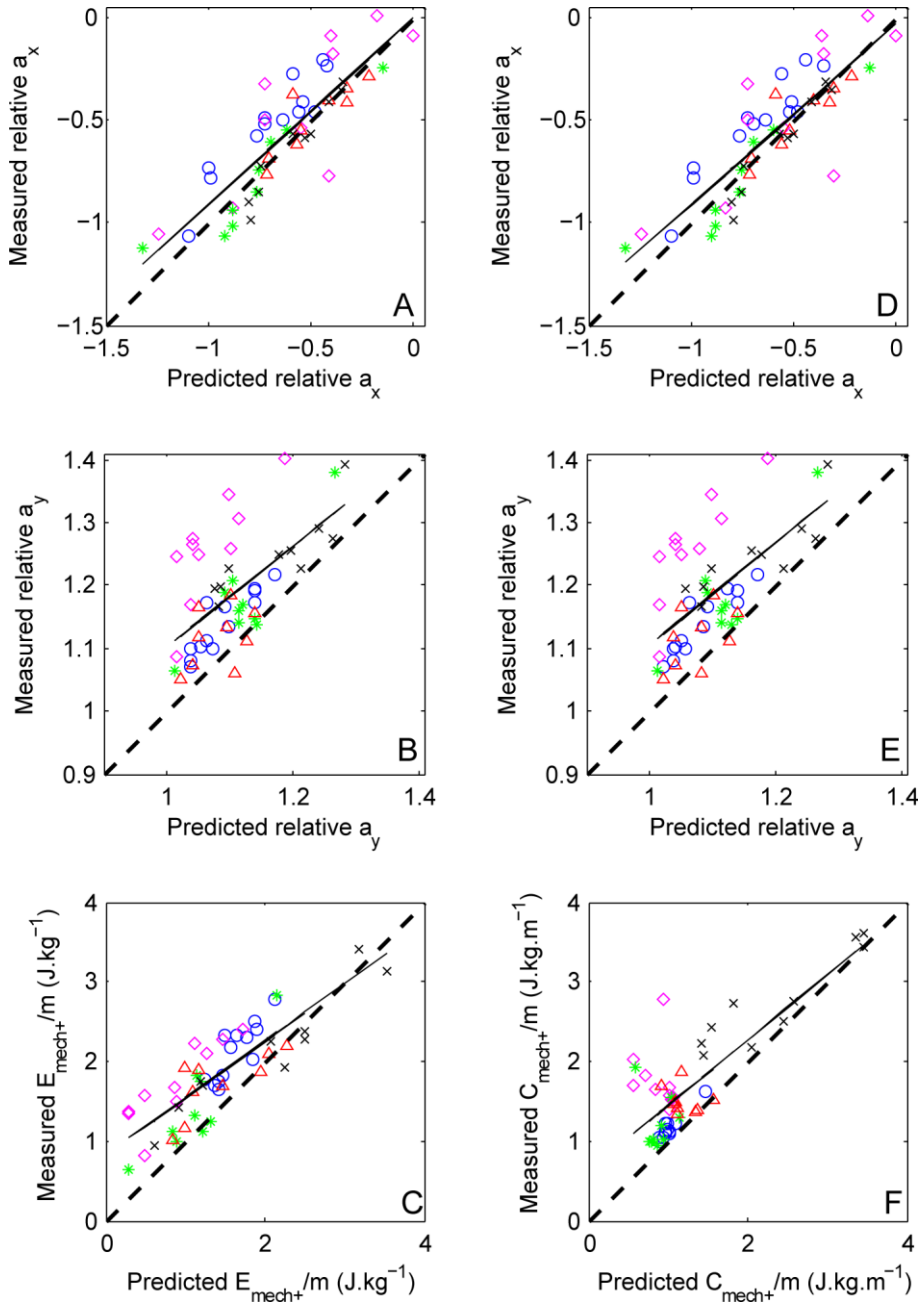

Figure 6: **Predicted and measures values.** Measured values of relative a_x (A), relative a_y (B) and E_{mech+}/m (C) plotted against calculated optimal values of these parameters for minimisation of E_{mech+}/m; measured values of relative a_x (D), relative a_y (E) and C_{mech+}/m (F) plotted against calculated optimal values of these parameters for minimisation of C_{mech+}/m. Results are for all trials and all dogs, with each dog's data points indicated by a different symbol. The fitted linear regression line is shown as a black solid line; the black broken line indicates the line of equality (x=y). r^2 values are 0.72 (A), 0.39 (B), 0.71 (C), 0.72 (D), 0.41 (E), 0.66 (F).

TABLES

Subject	Age (years)	Breed/type	Sex	Mass (kg)	Standing greater trochanter height (m)
P1	1.9	Working cocker spaniel	F	12.05	0.35
P2	4	Lurcher	M	19.00	0.46
P3	8	Lurcher	M	27.55	0.56
P4	1.2	Beauceron	M	36.90	0.55
P5	4	English springer spaniel	F	15.90	0.40

Table 1. Canine subject information.

Subject	Obstacle height (m)	Effective obstacle height (m)	Effective obstacle height as a proportion of hip height	Range of > 0 obstacle lengths (m) at 0.1 m intervals	Total number of trials performed
P1	0.35	0.47	1.34	0.10 - 1.00	12
P2	0.55	0.69	1.50	0.33 - 1.43	14
P3	0.48	0.71	1.27	0.48 - 1.38	12
P4	0.55	0.82	1.49	0.40 - 1.30	12
P5	0.40	0.56	1.40	0.20 - 1.10	12

Table 2. Height and lengths of the obstacles traversed. Each dog performed two additional trials with an obstacle length of 0.

Figure S1. Measured (○) and predicted (*) energy (E_{mech+}/m; left panel), CoM apex x position (a_x; middle panel) and CoM apex y position (a_y; right panel) plotted against CoM x position at take-off (d_x) for individual dogs. Each row of panels presents results from one dog (P1 top row --> P5 bottom row). Measured and predicted values for each jump are connected by a vertical line (red if measured value of parameter greater than predicted value; green if predicted value of parameter greater than measured value)

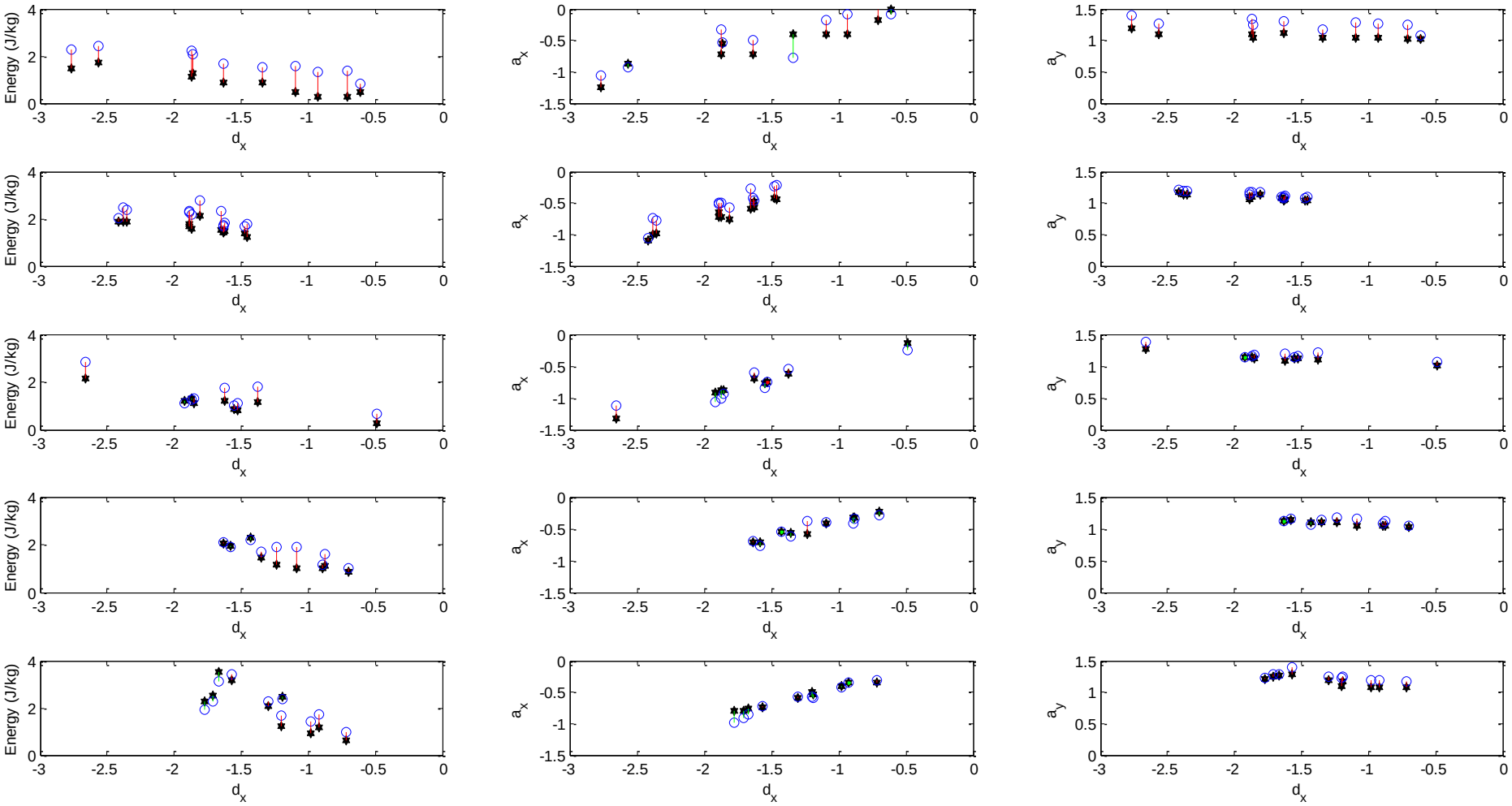

Figure S2. Measured (○) and predicted (*) cost of transport (C_{mech+}/m; left panel), CoM apex x position (a_x; middle panel) and CoM apex y position (a_y; right panel) plotted against CoM x position at take-off (d_x) for individual dogs. Each row of panels presents results from one dog (P1 top row --> P5 bottom row). Measured and predicted values for each jump are connected by a vertical line (red if measured value of parameter greater than predicted value; green if predicted value of parameter greater than measured value)

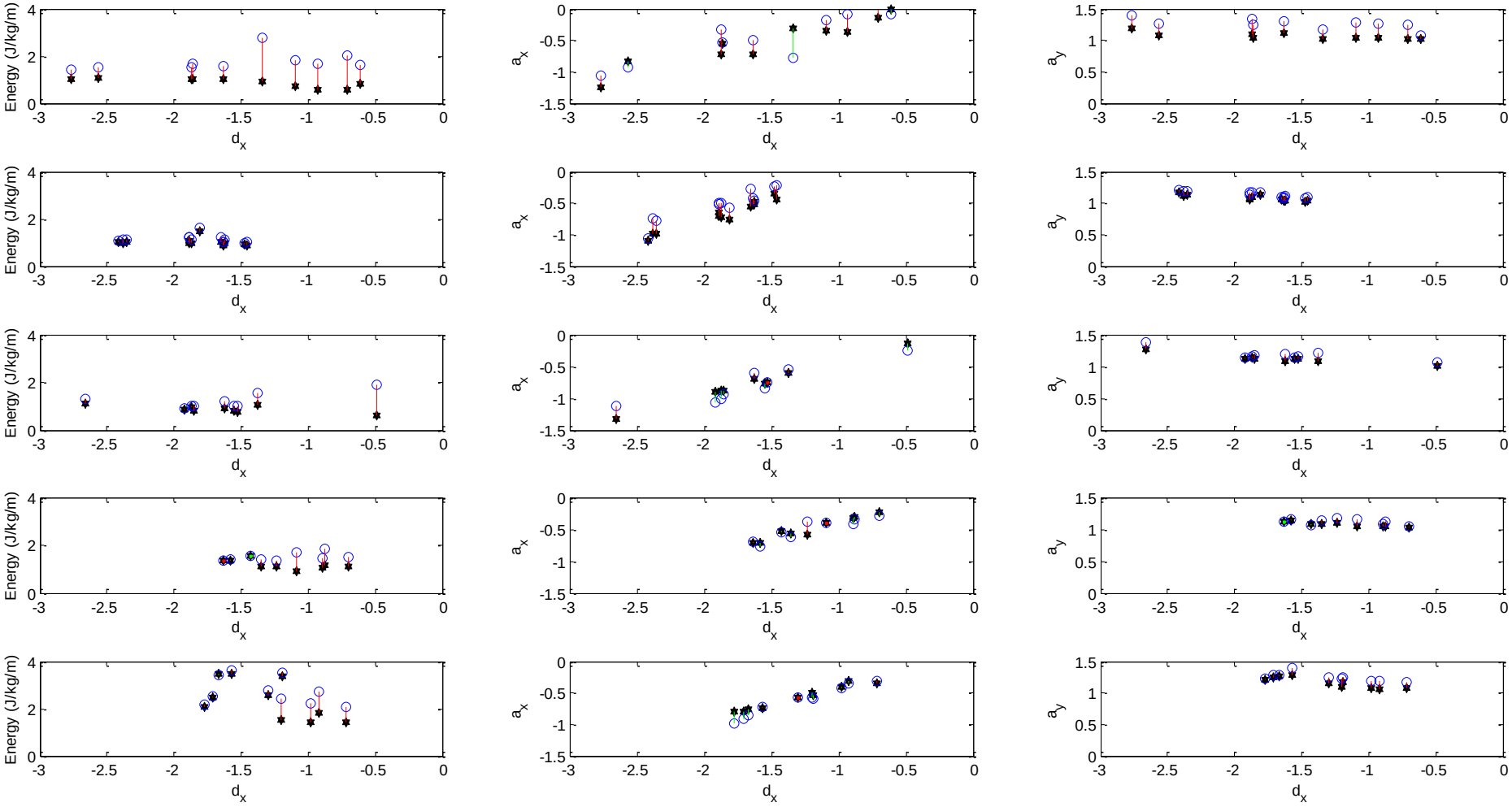

Data set

Click here to Download Data set

Journal of Experimental Biology • Supplementary information